

Enhanced $0_{g.s.}^+ \rightarrow 2_1^+$ $E2$ transition strength in ^{112}Sn

R. Kumar,^{1,*} P. Doornenbal,² A. Jhingan,¹ R. K. Bhowmik,¹ S. Muralithar,¹ S. Appannababu,³ R. Garg,⁴ J. Gerl,⁵ M. Górska,⁵ J. Kaur,⁶ I. Kojouharov,⁵ S. Mandal,⁴ S. Mukherjee,³ D. Siwal,⁴ A. Sharma,⁷ Pushpendra P. Singh,⁸ R. P. Singh,¹ and H.-J. Wollersheim⁵

¹Inter-University Accelerator Centre, New Delhi 110067, India

²RIKEN Nishina Center for Accelerator-Based Science, Wako, Saitama 351-0198, Japan

³Department of Physics, M.S. University of Baroda, Vadodara 390002, India

⁴Department of Physics & Astrophysics, University of Delhi, Delhi 110007, India

⁵Helmholtzzentrum für Schwerionenforschung GmbH, D-64291 Darmstadt, Germany

⁶Department of Physics, Panjab University, Chandigarh 160014, India

⁷Department of Physics, Bareilly College, Bareilly 243005, India

⁸INFN-Laboratori Nazionali di Legnaro (LNL), I-35020 Legnaro (PD), Italy

(Received 11 September 2009; published 8 February 2010)

Two consecutive Coulomb excitation experiments were performed to excite the 2_1^+ states of $^{112,116}\text{Sn}$ using a ^{58}Ni beam. For ^{112}Sn a $B(E2\uparrow)$ value of $0.242(8) e^2 b^2$ has been determined relative to the known value of ^{116}Sn . The present value is more precise than previous measurements and shows a clear discrepancy from the expected parabolic dependence between the doubly magic nuclei ^{100}Sn and ^{132}Sn . It implies that the reduced transition probabilities are not symmetric with respect to the midshell mass $A = 116$.

DOI: [10.1103/PhysRevC.81.024306](https://doi.org/10.1103/PhysRevC.81.024306)

PACS number(s): 23.20.Js, 21.10.Re, 25.70.De, 27.60.+j

I. INTRODUCTION

Numerous experimental and theoretical studies are currently focused on nuclear shell structure far from the line of stability (Ref. [1] and references therein). In particular, the evolution of nuclear properties, for example, the reduced transition probabilities across the $Z = 50$ chain of tin isotopes, has been examined in detail. This constitutes the longest shell-to-shell chain of semimagic nuclei investigated in nuclear structure to date. Radioactive ion beams yield new experimental results close to the doubly magic ^{100}Sn and ^{132}Sn , but very accurate data on the stable midshell nuclei are also of great relevance for our understanding of nuclear structure.

A simple shell model approach to investigating the characteristics of Sn isotopes is to consider ^{100}Sn as an inert core and to treat only neutron degrees of freedom, using the single-particle orbits of the $N = 50$ –82 shell as model space, that is, the five orbits $1g_{7/2}$, $2d_{5/2}$, $2d_{3/2}$, $3s_{1/2}$, and $1h_{11/2}$. Extensive shell model calculations have been performed using this approach [2]. Figure 1 shows the partial level schemes of even- A Sn isotopes with the dominating 6^+ and 10^+ yrast isomers resulting from the filling of the $g_{7/2}$ and $h_{11/2}$ neutron subshells in $A = 102$ –114 and $A = 116$ –130, respectively. These two regions seem to be divided by a soft closed subshell at $N = 64$. If spectroscopic properties of nuclei with more than six or eight valence neutrons are studied with the shell model, the required model space is, however, already exceedingly large. It is therefore appropriate to resort to further simplifications.

In semimagic nuclei, such as Sn isotopes, the seniority scheme provides a very valuable tool for describing low-energy spectra. The nearly constant energy of the first excited 2_1^+ state between $N = 52$ and $N = 80$ [3] is one of the well-

known features of Sn isotopes and is well explained within the generalized seniority model [4]. This seems to indicate that only one of the two kinds of nucleons contributes to the low-energy states. As a consequence, only the isovector ($T = 1$) interaction plays a leading role outside the doubly magic core, which cannot generate quadrupole deformation [5]. Furthermore, according to this theory, the electromagnetic transition rates between the 0^+ ground and the first excited 2_1^+ state exhibit parabolic behavior as a function of mass number across the Sn isotope chain. Thus, for a seniority changing transition, the $B(E2\uparrow)$ values increase at first, peak at midshell ($A = 116$), and fall off thereafter.

The experimental $B(E2; 0_{g.s.}^+ \rightarrow 2_1^+)$ values, henceforth $B(E2\uparrow)$, on the neutron-rich side of the Sn chain follow the theoretical predictions, as can be seen in Fig. 4. For the mass range $A = 116$ –130, the first excited 2_1^+ (seniority $\nu = 2$) state is generally an admixture of different neutron configurations, in contrast to the pure neutron $(h_{11/2})^n$ configuration for the long-lived 10^+ isomeric state. For lighter Sn isotopes, where the neutrons are filling the almost-degenerate single-particle $1g_{7/2}$ and $2d_{5/2}$ states, one observes an unexpected asymmetry in $E2$ strengths with respect to the heavier isotopes. This might indicate that the effective charge values depend on the orbit occupied by the nucleon. Two stable tin isotopes, ^{112}Sn and ^{114}Sn , yield higher $B(E2\uparrow)$ values than expected from shell model calculations, but so far large experimental errors have prohibited further theoretical interpretations. One should also note that the $B(E2\uparrow)$ value obtained for the unstable ^{108}Sn [6] in a Stopped Rare Isotope Spectroscopic INvestigation at GSI (RISING) experiment is based on a measurement relative to ^{112}Sn .

II. MOTIVATION AND EXPERIMENTAL DETAILS

The large uncertainty in the $B(E2\uparrow)$ values in ^{112}Sn and ^{114}Sn motivated two Coulomb excitation experiments to

* rakuiiac@gmail.com

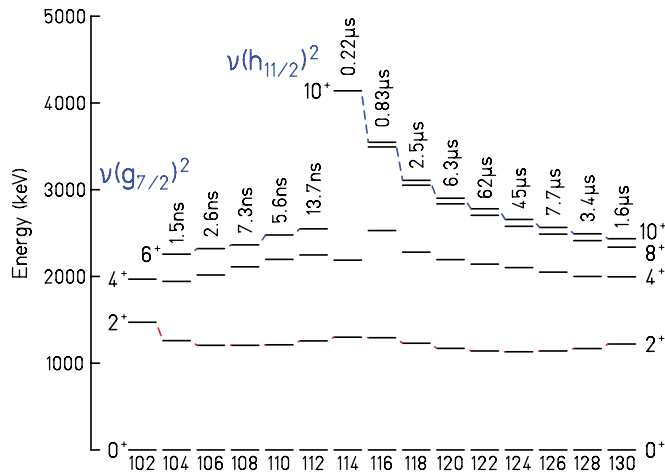


FIG. 1. (Color online) Partial level schemes [12] and isomer systematics in even- A Sn nuclei for mass numbers between $A = 102$ and $A = 130$. Levels of the same spin and positive parity are connected by dashed lines.

improve these crucial data points. In a previous measurement, the $B(E2\uparrow)$ value of ^{114}Sn was determined at the GSI (Helmholtzzentrum für Schwerionenforschung GmbH) [7]. The result showed an unexpected enhancement relative to the $B(E2\uparrow)$ of ^{116}Sn . This paper reports the results of a Coulomb excitation experiment and the measurement of the corresponding $B(E2\uparrow)$ value for ^{112}Sn . The literature value [3] for ^{112}Sn is mainly based on two rather accurate measurements [8,9], which differ by more than 11%. As there is no explanation given for the discrepancy [9], a detailed study of the reduced transition probabilities for the tin isotopes requires an additional measurement. The present experiment was performed at the Inter-University Accelerator Centre (IUAC) in New Delhi. Two targets, ~ 0.53 mg/cm 2 ^{112}Sn (99.5% enriched) and ^{116}Sn (98% enriched), were bombarded with ^{58}Ni ions at an incident energy of 175 MeV, which is well below the Coulomb barrier, to ensure pure electromagnetic interaction. In two consecutive experiments the relative excitation strength of the 2^+ state in ^{112}Sn and ^{116}Sn was determined, with the first excited 2^+ state in ^{58}Ni used for normalization. This ensured that systematic errors were excluded and the projectile excitation canceled in the $^{112}\text{Sn}/^{116}\text{Sn}$ γ -ray yield ratio. The γ -ray ratio is a direct measure of the $B(E2\uparrow)$ of ^{112}Sn relative to that of ^{116}Sn . Because the adopted $B(E2\uparrow)$ value for ^{116}Sn , $0.209(6) e^2 b^2$, is an evaluation of 11 different experimental results [3], it becomes a reliable and precise reference point.

Scattered projectiles and recoils were detected in an annular gas-filled parallel-plate avalanche counter (PPAC), subtending the angular range $15^\circ \leq \vartheta_{\text{lab}} \leq 45^\circ$ in the forward direction. This detector was placed 11 cm from the target and was position sensitive in both the azimuthal and the polar angles. The azimuthal angle φ was obtained from the anode foil, which was divided into 20 radial sections of 18° each. To measure the polar angle ϑ , the cathode was patterned in concentric conductor rings, each 1 mm wide, with an insulating gap of 0.5 mm between them. Each ring was connected to its neighbor by a delay line of 2 ns. The cathode signals were read out from

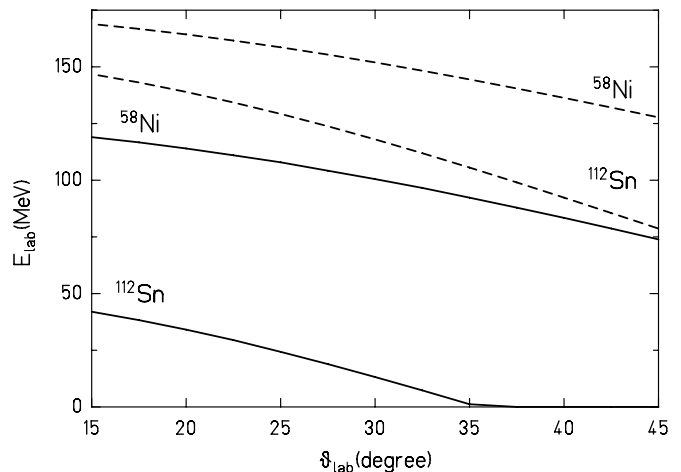


FIG. 2. Kinetic energies of scattered ^{58}Ni projectiles and ^{112}Sn recoils detected in the angular range of 15° to 45° covered by the PPAC. Dashed lines are based on two-body kinematics for a beam energy of 175 MeV, whereas solid lines are corrected for energy loss [10] in a $10\text{-}\mu\text{m}$ Mylar foil, which was used as the entrance window of the PPAC.

the innermost and outermost rings, and the ϑ information was derived from the time difference between the anode and the cathode signals. For technical reasons, only 14 of the anode segments were used in the experiment. An entrance window of $10\text{-}\mu\text{m}$ -thick Mylar was used for the PPAC, which reduced the kinetic energy of both reaction partners. Whereas ^{58}Ni projectiles could still be measured in the PPAC, Sn recoils either were stopped in the entrance window or were close to the detection limit. Figure 2 shows qualitatively the effect of $10\text{-}\mu\text{m}$ -thick Mylar foil on the kinetic energy of both reaction partners. In this way distant collisions (Ni detected in PPAC) could be distinguished from close collisions (Sn detected).

De-excitation γ -rays were detected in four clover detectors mounted at $\vartheta_\gamma \sim 135^\circ$ with respect to the beam direction at a distance of ~ 22 cm to the target. The φ_γ angles for the clover detectors were $\pm 55^\circ$ and $\pm 125^\circ$ with respect to the vertical direction. Individual energies of the 16-Ge crystals and common timing signals of the four clover detectors were recorded in coincidence with the PPAC anode and cathode signals event by event. Low-energy radiations were suppressed using Cu, Sn, and Pb absorbers of thicknesses between 0.5 and 0.7 mm placed in front of the clover detectors. To avoid any systematic error, the ^{112}Sn and ^{116}Sn targets were used in turn every 3 h, for a total measuring time of approximately 50 h. Energy and relative efficiency calibrations were carried out using a ^{152}Eu source.

III. DATA ANALYSIS AND RESULT

The particle identification and the particle position measurement allowed for a precise Doppler correction of the measured γ -ray energies. From the measured (ϑ, φ) angle of the scattered Ni projectiles, the velocities of both reaction partners and the recoil angles could be calculated from two-particle kinematics. In the analysis, an add-back procedure (applied to

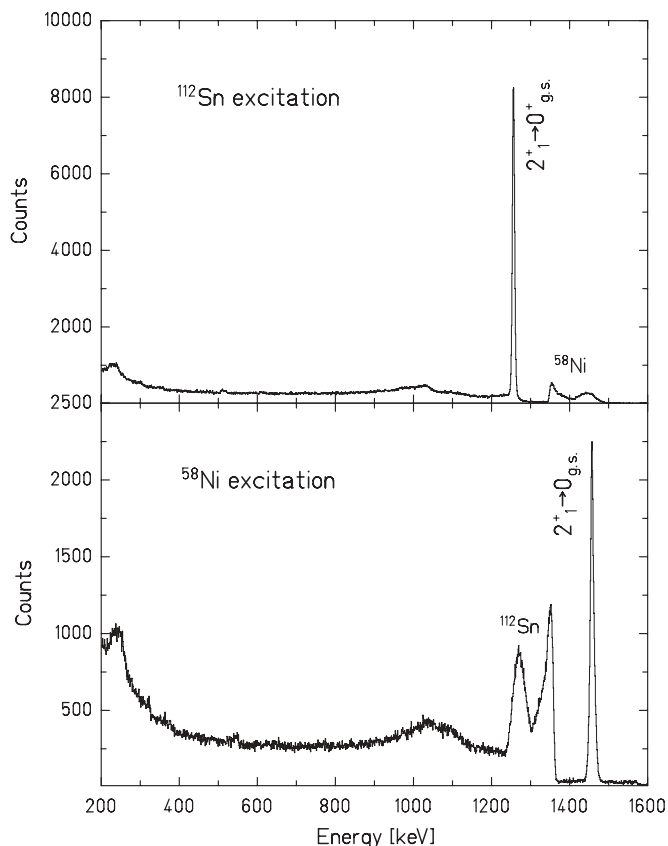


FIG. 3. Doppler-corrected γ -ray spectra emitted from ^{112}Sn target nuclei (top) and ^{58}Ni projectiles (bottom) in the reaction $^{112}\text{Sn}(^{58}\text{Ni}, ^{58}\text{Ni}^*)^{112}\text{Sn}$ at 175 MeV. Scattered ^{58}Ni projectiles were detected in the PPAC and clover detectors were operated in the add-back mode.

all four crystals within each Ge clover) and a Doppler shift correction were performed for each clover detector ($\vartheta_\gamma, \varphi_\gamma$) event by event. Figure 3 shows the Doppler-corrected spectra for ^{112}Sn excitation (top) and ^{58}Ni excitation (bottom) with the dominating $2_1^+ \rightarrow 0_{g.s.}^+$ transitions. Higher excited states were not observed. A γ -ray resolution of 13 keV (full width at half-maximum; FWHM) was obtained for target excitation, and 7 keV (FWHM) for projectile excitation, which results from the finite solid angle of the γ -ray detector (intrinsic resolution, <3 keV).

From observation of the Doppler-corrected γ -ray lines corresponding to $2_1^+ \rightarrow 0_{g.s.}^+$ transitions, the target and projectile excitation can be extracted. The $B(E2\uparrow)$ value of ^{112}Sn was obtained from the experimental γ -ray intensity double ratio $[I_\gamma(^{112}\text{Sn})/I_\gamma(^{58}\text{Ni})]/[I_\gamma(^{116}\text{Sn})/I_\gamma(^{58}\text{Ni})]$ of the $2_1^+ \rightarrow 0_{g.s.}^+$ decays. This double ratio was corrected for the different Ge detector efficiency (1.7%) and target enrichments (1.5%). Coulomb excitation calculations were performed with the Winther-de Boer Coulex code [11]. Calculations included the feeding contributions from the $0_2^+, 2_2^+, 3_1^-,$ and 4_1^+ states in ^{112}Sn and ^{116}Sn , which were obtained from the known excitation strengths given in Ref. [12]. In both cases the summed intensity from decays of higher-lying states added up to less than 2% of the $2_1^+ \rightarrow 0_{g.s.}^+$ decay intensity, which

agreed with our experimental findings. The calculated double ratio changed by less than 1% when the feeding states were neglected. The slowing-down of the projectiles in the targets (0.8%), the uncertainty of the PPAC boundaries (0.5%), and the adopted ^{116}Sn $B(E2\uparrow)$ value (3%) were also considered. In the second step, the γ -ray decay was calculated taking into account the particle- γ angular correlation (0.8%), the internal conversion, and the finite geometry of the γ detector. The $0_{g.s.}^+ \rightarrow 2_1^+$ matrix element in ^{112}Sn was adjusted in the Coulex calculations to reproduce the experimental double ratio. The resulting $B(E2\uparrow)$ value in ^{112}Sn is $0.242(8) e^2 b^2$. It is consistent with previous values [3,13,14] but has a higher precision. The error is the quadratic sum of the four individual uncertainties mentioned previously and the uncertainty of the γ -ray intensities (1%). Because the largest contribution to the error of ^{112}Sn and ^{114}Sn [7] results from the uncertainty of the $B(E2\uparrow)$ value in ^{116}Sn , the mass dependence was determined with an even higher accuracy. Moreover, the new result will influence the RISING data for ^{108}Sn that were deduced relative to the adopted value for ^{112}Sn . A renormalization using our new $B(E2\uparrow)$ value for ^{112}Sn leads to a value of $B(E2\uparrow) = 0.232(57) e^2 b^2$ for ^{108}Sn .

IV. DISCUSSION

The experimental information in the $B(E2\uparrow)$ systematics on tin isotopes with the new value of ^{112}Sn included is presented in Fig. 4 and listed in Table I. It is apparent that the result for ^{112}Sn is about 20% larger than that for ^{120}Sn , in contrast to the symmetric distribution expected with respect to the midshell $A = 116$. According to the seniority model the $B(E2\uparrow)$ values naturally decrease with a decreasing number of particles outside the closed core. This trend cannot be found in our data for ^{112}Sn and ^{114}Sn [7]. As the experimental $B(E2\uparrow)$ value already increases when

TABLE I. Comparison of measured $B(E2\uparrow)$ values for Sn isotopes with calculated data [18]. Experimental data on neutron-deficient isotopes are averaged values from Refs. [6] and [15–17].

Isotope	$E_{2_1^+}$ (keV)		$B(E2\uparrow) e^2 b^2$	
	Exp	RQRPA	Exp	RQRPA
^{102}Sn	1472.0(2)	1341		0.094
^{104}Sn	1260.1(3)	1001		0.185
^{106}Sn	1207.7(5)	891	0.209(32)	0.235
^{108}Sn	1206.1(2)	940	0.224(16)	0.227
^{110}Sn	1211.9(2)	1014	0.226(18)	0.202
^{112}Sn	1256.9(7)	1112	0.242(8)	0.176
^{114}Sn	1299.9(7)	1207	0.232(8)	0.155
^{116}Sn	1293.6(8)	1236	0.209(6)	0.144
^{118}Sn	1229.7(2)	1242	0.209(8)	0.146
^{120}Sn	1171.3(2)	1269	0.202(4)	0.150
^{122}Sn	1140.6(3)	1296	0.192(4)	0.152
^{124}Sn	1131.7(2)	1340	0.166(4)	0.145
^{126}Sn	1141.2(2)	1411	0.10(3)	0.126
^{128}Sn	1168.8(4)	1537	0.073(6)	0.096
^{130}Sn	1121.3(5)	1751	0.023(5)	0.055

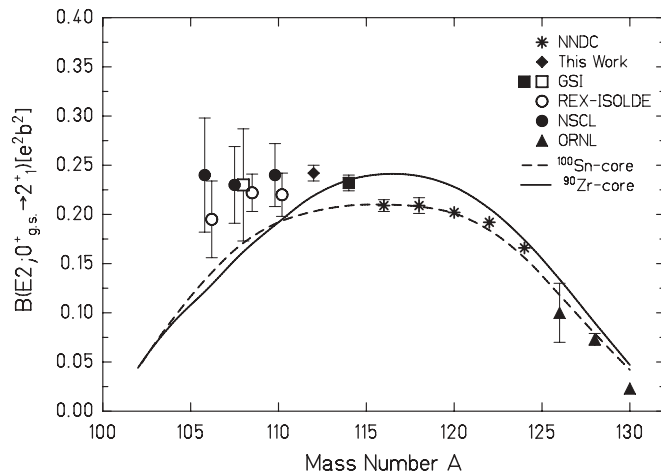


FIG. 4. Experimental data on $B(E2; 0_{g.s.}^+ \rightarrow 2_1^+)$ values in the Sn isotope chain from the current result for ^{112}Sn and from Refs. [3,6,7], and [15–17]. Dashed and solid lines show the predictions of the large-scale shell model calculations from Ref. [6] performed with a ^{100}Sn core and a ^{90}Zr core, respectively.

going from ^{116}Sn to ^{114}Sn , it appears that proton excitations play an important role in the transition. Banu *et al.* [6] include up to 4p-4h proton core excitations in their calculations by means of a seniority truncated model space outside of a ^{90}Zr core. Because of the seniority truncation in that calculation the systematic trend in $B(E2\uparrow)$ values was retained. The comparison between experiment and theory shows agreement for the heavier Sn isotopes assuming a ^{100}Sn core. However, for the lighter Sn isotopes asymmetry of the $B(E2\uparrow)$ systematics is observed. This indicates a different character of the core excitations in the $N = Z$ and $N > Z$ regions of the tin isotopic chain.

With reference to Fig. 1, as already pointed out, there seems to be a subshell closure at $N = 64$ for the Sn isotope chain. Below this boundary, the level structure is dominated by the $(d_{5/2})^2$ and $(g_{7/2})^2$ components, whereas the $(h_{11/2})^2$ component governs the heavier Sn decay schemes. Around $N = 64$, all single-particle configurations contribute approximately equally and yield an increased excitation energy of

the 2_1^+ states in ^{114}Sn and ^{116}Sn compared with the other Sn isotopes. However, reduced transition probabilities test nuclear structure in still greater detail than excitation energies, because the former involve the wave functions of the initial and final states.

Recently [18], the relativistic quasiparticle random-phase approximation (RQRPA) has been applied to calculate the energies of the first excited 2^+ states and corresponding $B(E2\uparrow)$ values for tin isotopes with even mass numbers $A = 100$ –134. The great advantage of this RQRPA scheme is that it is not necessary to assume an inert core and to adjust parameters of the Hamiltonian from nucleus to nucleus or region to region of the periodic table. In Table I we compare the measured $B(E2\uparrow)$ values of the Sn isotopes with the calculated data [18]. Considering that there is no free adjustment of parameters or effective charges, the agreement with the theoretical data is very good. The most important feature is the asymmetric behavior of the $B(E2\uparrow)$ data with respect to the midshell nucleus ^{116}Sn . It is interesting to note that the same RQRPA calculations yield quite satisfactory agreement also for the Ni and Pb isotopes [19].

In conclusion, the $B(E2; 0_{g.s.}^+ \rightarrow 2_1^+)$ value in stable ^{112}Sn was measured relative to the well-known result for ^{116}Sn in a Coulomb excitation experiment. The observation from the experimental $B(E2\uparrow)$ value increases upon going from ^{116}Sn to ^{112}Sn , which indicates that the generalized seniority scheme fails to describe the $B(E2\uparrow)$ systematics for Sn isotopes. The experimental data are also compared with RQRPA calculations that predict the observed asymmetric behavior of the $B(E2\uparrow)$ values with respect to the midshell nucleus with $N = 66$.

ACKNOWLEDGMENTS

The authors would like to thank N. Madhavan for many helpful discussions and S. K. Saini, A. Kotari, and R. Ahuja for their significant contribution to the experiment. Thanks go to the operating staff of the Inter-University Accelerator Centre (IUAC) accelerator for supplying the excellent Ni beam. This work was performed under IUAC-GSI collaboration. P.D. acknowledges the financial support given by the Japan Society for the Promotion of Science.

[1] H. Grawe and M. Lewitowicz, Nucl. Phys. **A693**, 116 (2001).
 [2] M. Hjorth-Jensen, T. T. S. Kuo, and E. Osnes, Phys. Rep. **261**, 125 (1995).
 [3] S. Raman, C. W. Nestor, and P. Tikkanen, At. Data Nucl. Data Tables **78**, 1 (2001).
 [4] I. Talmi, Nucl. Phys. **A172**, 1 (1971).
 [5] R. Casten, *Nuclear Structure from a Simple Perspective* (Oxford University Press, New York, 2000).
 [6] A. Banu *et al.*, Phys. Rev. C **72**, 061305(R) (2005).
 [7] P. Doornenbal *et al.*, Phys. Rev. C **78**, 031303(R) (2008).
 [8] P. H. Stelson *et al.*, Phys. Rev. C **2**, 2015 (1970).
 [9] R. Graetzer *et al.*, Phys. Rev. C **12**, 1462 (1975).

[10] L. C. Northcliffe and R. F. Schilling, Nucl. Data Tables **A 7**, 233 (1970).
 [11] A. Winther and J. de Boer, in *Coulomb Excitation*, edited by K. Alder and A. Winther (Academic Press, New York, 1966).
 [12] <http://www.nndc.bnl.gov/ensdf/>.
 [13] J. N. Orce *et al.*, Phys. Rev. C **76**, 021302(R) (2007).
 [14] J. N. Orce *et al.*, Phys. Rev. C **77**, 029902(E) (2008).
 [15] D. C. Radford *et al.*, Nucl. Phys. **A752**, 264c (2005).
 [16] J. Cederkäll *et al.*, Phys. Rev. Lett. **98**, 172501 (2007).
 [17] A. Ekström *et al.*, Phys. Rev. Lett. **101**, 012502 (2008).
 [18] A. Ansari, Phys. Lett. **B623**, 37 (2005).
 [19] A. Ansari and P. Ring, Phys. Rev. C **74**, 054313 (2006).